

RESEARCH ARTICLE

Proteomic analysis enables distinction of early- versus advanced-stage lung adenocarcinomas

Olga Kelemen¹ | Indira Pla^{1,2}  | Aniel Sanchez^{1,2} | Melinda Rezeli¹ | Attila Marcell Szasz^{1,3,5,6} | Johan Malm^{2,6} | Viktoria Laszlo^{4,6} | Ho Jeong Kwon^{1,5} | Balazs Dome^{4,6,7} | Gyorgy Marko-Varga¹

¹ Clinical Protein Science and Imaging, Biomedical Center, Department of Biomedical Engineering, Lund University, Lund, Sweden

² Department of Translational Medicine, Lund University, Malmö, Sweden

³ Cancer Center, Semmelweis University, Budapest, Hungary

⁴ Department of Surgery, Division of Thoracic Surgery, Comprehensive Cancer Center Medical University of Vienna, Vienna, Austria

⁵ Chemical Genomics Global Research Lab, Department of Biotechnology, College of Life Science and Biotechnology, Yonsei University, Seoul, Republic of Korea

⁶ Department of Tumor Biology, National Korányi Institute of Pulmonology, Budapest, Hungary

⁷ Department of Thoracic Surgery, Semmelweis University and National Institute of Oncology, Budapest, Hungary

Correspondence

Gyorgy Marko-Varga, Clinical Protein Science and Imaging, Biomedical Center, Department of Biomedical Engineering, Lund University, Lund, Sweden.

Email: gyorgy.marko-varga@bme.lth.se

Balazs Dome, Department of Surgery, Division of Thoracic Surgery, Comprehensive Cancer Center, Medical University of Vienna, Austria.

Email: balazs.dome@meduniwien.ac.at

Olga Kelemen and Indira Pla contributed equally to this work.

Balazs Dome and Gyorgy Marko-Varga are co-senior authors (*)

Funding information

National Research Foundation of Korea, Grant/Award Numbers: 2015K1A1A2028365, 2016K2A9A1A03904900, KNN121510, NVKP_16-1-2016-0042; National Research, Development and Innovation Office of Hungary; Hungarian National Research, Development and Innovation Office, Grant/Award Numbers: KH130356, K129065

Abstract

Background: A gel-free proteomic approach was utilized to perform in-depth tissue protein profiling of lung adenocarcinoma (ADC) and normal lung tissues from early and advanced stages of the disease. The long-term goal of this study is to generate a large-scale, label-free proteomics dataset from histologically well-classified lung ADC that can be used to increase further our understanding of disease progression and aid in identifying novel biomarkers.

Methods and results: Cases of early-stage (I-II) and advanced-stage (III-IV) lung ADCs were selected and paired with normal lung tissues from 22 patients. The histologically and clinically stratified human primary lung ADCs were analyzed by liquid chromatography-tandem mass spectrometry. From the analysis of ADC and normal specimens, 4863 protein groups were identified. To examine the protein expression profile of ADC, a peak area-based quantitation method was used. In early- and advanced-stage ADC, 365 and 366 proteins were differentially expressed, respectively, between normal and tumor tissues (adjusted P -value < .01, fold change ≥ 4). A total of 155 proteins were dysregulated between early- and advanced-stage ADCs and 18 were suggested as early-specific stage ADC. In silico functional analysis of the upregulated proteins in both tumor groups revealed that most of the enriched pathways are involved in mRNA metabolism. Furthermore, the most overrepresented pathways in the proteins that were unique to ADC are related to mRNA metabolic processes.

This is an open access article under the terms of the [Creative Commons Attribution](https://creativecommons.org/licenses/by/4.0/) License, which permits use, distribution and reproduction in any medium, provided the original work is properly cited.

© 2020 The Authors. *Clinical and Translational Medicine* published by John Wiley & Sons Australia, Ltd on behalf of Shanghai Institute of Clinical Bioinformatics

Conclusions: Further analysis of these data may provide an insight into the molecular pathways involved in disease etiology and may lead to the identification of biomarker candidates and potential targets for therapy. Our study provides potential diagnostic biomarkers for lung ADC and novel stage-specific drug targets for rational intervention.

KEYWORDS

clinical proteomics, lung adenocarcinomas, mass spectrometry, proteomics

1 | INTRODUCTION

Lung cancer is today one of the leading causes of cancer deaths worldwide. Despite a poor 5-year survival rate of 15%, no improvement in survival has occurred for decades.¹ Nonsmall cell lung cancer (NSCLC) is subdivided into three major histological types: squamous cell carcinoma, large cell carcinoma, and adenocarcinoma (ADC). ADC of the lung is the predominant histological type of lung cancer and accounts for 40% of all NSCLC cases. Although lung ADC is associated with smoking, it is the most frequent lung malignancy in individuals who have never smoked.²

Traditionally, therapeutic strategies for NSCLC are based on tumor histology and stage. At the early stage, surgical resection is the most effective treatment. The standard first-line therapy for patients with inoperable, advanced NSCLC has been to employ different chemotherapy modalities. Although specific molecular-targeted therapies for the treatment of distinct subtypes of NSCLC have been developed, treatment options for the majority of patients remain unsatisfactory. Therefore, new treatment strategies with greater efficacy and lower toxicity are essential. Additionally, both diagnostic and prognostic biomarkers are urgently required to increase patient survival.

Recent advancements in high-throughput molecular biology technologies have deepened our understanding of the pathology underlying NSCLC and highlighted the significant heterogeneity of NSCLC.³ Sequencing of entire cancer genomes has resulted in the identification of driver mutations and frequently altered signaling pathways. This approach has led to the definition of new molecular subtypes of NSCLC (EGFR, ALK, TP53, KRAS, and ROS1) and new treatment options.⁴⁻⁷

The prognosis for lung cancer patients is strongly related to the stage of the disease at the time of diagnosis. Patients with localized disease have a 5-year survival rate of 52%, meanwhile, patients diagnosed with the distal disease have a dismal 5-year survival rate of 3.6%.² Only one third of lung cancer cases, however, are diagnosed at an early stage.⁸ Therefore, early diagnosis plays a crucial role in reduc-

ing lung cancer mortality. The current screening methods mainly include the histopathological examination of biopsies, lung imaging, and biochemical screens for several specific biomarkers. Several potential biomarkers have already been identified. These include the genes CEA, CYFRA21-1, KRAS, and TP53⁹; however, the majority of these biomarkers fail to show a strong specificity and sensitivity for early-stage lung cancer.

Proteins are implicated in all biological processes; thus, these play an essential role in disease progression. Therefore, large-scale and systematic analyses of proteins have become an important tool for tumor characterization. Proteomic methods based on mass spectrometry (MS) have emerged as powerful tools to discover diagnostic, prognostic, and therapeutic protein biomarkers.¹⁰ Various MS-based approaches have been used to identify differentially expressed proteins (DEPs) in lung ADC cells, tissues, and biological fluids.¹¹ Due to the low cost, minimal sample handling and manipulation, and high throughput, the application of label-free proteomics to investigate differential protein expression of clinical samples has gained considerable attention.

Fresh tissue is difficult to collect for clinical proteomic studies; therefore, FFPE (formalin-fixed and paraffin-embedded) tissues are the most frequently used and are easily preserved for subsequent clinical diagnoses. FFPE tissues are routinely collected for clinical diagnosis; however, due to the presence of formalin-induced protein crosslinks and modifications,¹² protein recovery from FFPE tissues is difficult. Proteomic analysis of fresh frozen tissues may reflect more accurately the *in vivo* tissue proteome. Therefore, surgically resected fresh frozen tissues were used in this study.

Label-free, gel-free proteomics has been widely used to describe large-scale biological systems.¹³ Label-free MS-based proteomic methods provide relative protein abundance in normal and cancer tissues that may aid in obtaining a deeper insight into molecular interactions, signaling pathways, and biomarker identification. In the current study, a proteomic analysis was conducted using a label-free liquid chromatography (LC)-MS approach to

systematically assess the stage-specific signaling pathways and potential markers. This enabled high-throughput, semiquantitative assessment of protein abundances in a complex mixture. These results provide a deeper insight into the proteomes of early- and advanced-stage lung ADC.

2 | MATERIALS AND METHODS

2.1 | Sample selection

We collected malignant and adjacent nonmalignant lung tissue samples from 22 patients between 46 and 74 years old (median: 60 years) with ADC histology. Out of 22, 11 patients were in the early-stage of ADC (pathological stage I and II disease) and 11 had advanced-stage ADC (pathological stage III and IV disease) (Table 1). Malignant and adjacent nonmalignant lung tissue samples were harvested in the operating theater from patients undergoing resection or lobectomy for NSCLC. The matched control lung tissue was excised from regions that were distant (8-10 cm) from the tumor. All procedures were approved by institutional IRB (2521-0/2010-1018EKU) protocols with informed patient consent. Tissue samples were promptly frozen in liquid nitrogen and stored at -80°C . Specimens were annotated with age, gender, race, diagnosis (including stage), smoking status, and the number of pack years. Criteria for patient selection were as follows: current or former smokers; diagnosis of NSCLC ADC; early stage (I-II) or advanced stage (III-IV) (Table 1). Detailed information of each patient and Hematoxylin and Eosin (H&E) images can be accessed in Supplementary File F1.

2.2 | Sample preparation

Preparation of tissues followed by protein extraction using buffer exchange was performed as previously described.¹⁴ In brief, frozen tissue samples from each tumor were sliced into $10 \times 10 \mu\text{m}$ sections using a cryotome. Tissue sections were then homogenized in lysis buffer (50 mM ammonium bicarbonate, 6 M urea) and incubated for 30 min on ice. Samples were sonicated, clarified by centrifugation for 10 min ($10\,000 \times g$, 4°C), and the supernatant transferred to a clean microcentrifuge tube. Total protein concentration was determined using the BCA protein assay kit (Pierce, Thermo Fischer Scientific). Proteins were reduced with 10 mM Dithiothreitol (DTT) (1 h at 37°C) and alkylated using 40 mM iodoacetamide (30 min, in the dark at room temperature) followed by buffer exchange with 50 mM ammonium bicarbonate buffer (pH 7.6). A total of 50 μg total protein was digested overnight at 37°C with trypsin at an enzyme to

Graphical Highlights

1. Mass spectrometry analysis revealed changes at the protein level between early- and advanced-stage lung adenocarcinomas.
2. Most of the protein-enriched pathways overexpressed in tumor ADCs are involved in mRNA metabolism.
3. The proteomics analysis identified 18 early-specific proteins.
4. Potential diagnostic biomarkers were identified for lung ADC and novel stage-specific drug targets for rational intervention.

protein ration of 1:50 w/w. The digested peptides were concentrated and desalted with C18 MicroSpin columns, and lyophilized and resuspended in 0.1% formic acid +5 fmol/ μL PRTC (Pierce Peptide Retention Time Calibration Mixture).

2.3 | Proteomic analysis and database searching

Samples (peptides produced by digestion) were analyzed by triplicate in a randomized order using a Q-Exactive Plus mass spectrometer connected to an Easy-nLC 1000 pump (Thermo Scientific, San José, CA) with a top 10 DDA method (2 μL , 1 μg on the column). Peptides were loaded onto an Acclaim PepMap 100 precolumn ($75 \mu\text{m} \times 2 \text{ cm}$, Thermo Scientific), and separated on an easy-Spray column ($25 \text{ cm} \times 75 \mu\text{m ID}$, PepMap C18 2 μm , 100 \AA) with the flow rate set to 300 nL/min and the column temperature to 35°C . A nonlinear 90 min gradient was applied, using solvent A (0.1% formic acid) and solvent B (0.1% formic acid in acetonitrile). Full MS scans were acquired with the Orbitrap mass analyzer over m/z 400-1600 range and the Target Automated Gain Control (AGC) value was set to 1×10^6 and maximum injection time of 100 ms. The 10 most intense peaks with charge state ≥ 2 were fragmented in the Higher-energy Collisional Dissociation (HCD) collision cell with a normalized collision energy of 26%. Tandem mass spectra were acquired in the Orbitrap mass analyzer with a resolution of 17 500 (at m/z 200), target AGC value of 5×10^4 and maximum injection time of 100 ms. The underfill ratio was set to 10% and dynamic exclusion was 45 s.

Raw files were analyzed with Proteome Discoverer v2.1 (Thermo Scientific). Proteins were searched against the UniProtKB human database using the SEQUEST HT

TABLE 1 Patient characteristics

Characteristics	n (%)
Total number of patients	22 (100%)
Sex	
Female	13 (59.1%)
Male	9 (40.9%)
Age at the diagnosis, years	
Median (range)	60 (46-74)
<60	9 (40.9%)
≥60	13 (59.1%)
Smoker	
Current smoker	10 (45.5%)
Former smoker	11 (50 %)
Unknown	1 (4.5%)
T stage	
T1	5 (22.7%)
T2	13 (59.1%)
T3	4 (18.2%)
N stage	
N0	10 (45.5%)
N1	4 (18.2%)
N2	8 (36.3%)
Disease stage	
Ia (early)	4 (18.2%)
IIa (early)	4 (18.2%)
IIb (early)	3 (13.6%)
IIIa (advanced)	9 (40.9%)
IV (advanced)	2 (9.1%)

search algorithm that is integrated into Proteome Discoverer. The search was performed with the following parameters: carbamidomethylation of cysteine residues and oxidation of methionine residues as static and dynamic modifications, respectively; and mass tolerances of 10 ppm for precursor ion and 0.02 Da for fragment ions. Up to two missed cleavages for tryptic peptides were allowed. The filters “high confidence” and “at least two unique peptides per protein” were also applied (false discovery rate [FDR] < .01).

Peptide and protein quantitation was assessed using the converted mxml files¹⁵ (MSconvert) and analyzed by OpenMS v.2.0.0 and TOPP¹⁶ using X-tandem as search engine against the UniProt human database (Human, 9606; reviewed, 20 165). The search included carbamidomethylation of cysteine residues and oxidation of methionine residues as static and dynamic modifications, respectively. FDR was determined by searching a reversed database and was set to < .01 for proteins and peptides (at least two unique peptides/protein). Enzyme specificity was “trypsin” and ‘two miscleavages’ were permitted with

a minimum of seven amino acids per identified peptide. Peptide identification was based on a search with an initial mass deviation for the precursor and fragment ions of up to 10 ppm and 0.02 Da, respectively. To match peptide identifications across different replicates and adjacent samples by condition, a match-between-runs was performed.

For the quality control (QC) of the LC-MS analysis, four of the most intense peaks observed in all LC-MS runs of previous analyses performed in our laboratory with lung tissues samples were selected as QC reference (see Table F1-S1 of the File F2 in the Supporting Information). In addition, mass error distribution for peptide groups and the distribution of peptide by retention times across the LC-MS is showed. See the results of the analysis in File F2 in the Supporting Information.

2.4 | Bioinformatics

Statistical analyses and data visualization were performed in Perseus¹⁷ (v1.6.0.2) and R.^{18,19} In order to obtain >70% valid values per protein in at least one condition, data were filtered based on missing values. Missing values were replaced using a “data imputation” algorithm to simulate signals of low-abundance proteins under the assumption that these are biased toward the detection limit of the MS measurement. In Perseus, a width of 0.3 and a downshift of 1.8 were chosen to draw random numbers from a normal distribution. The intensities were normalized by applying a log₂ transformation and then standardized by subtracting the median. An overall picture of the proteomics results was assessed by performing a principal component analysis (PCA)^{20,21} based on the expression of all proteins quantified in all samples. To determine DEPs, an ANOVA test was initially performed to detect changes across the four sample groups. To compare normal and tumor tissues within the disease stages, a paired Student *t*-test (two-tailed) was then performed; and to compare tissues of early versus advanced stages, an unpaired Student *t*-test (two-tailed) was applied. In all cases, *P*-values were adjusted to obtain a FDR < 1%. Proteins with *q*-values < .01 and fold change (FC) ≥ 4 were considered differentially expressed. To visualize the behavior of DEPs across the time points, unsupervised hierarchical clustering (distance: “euclidean”; linkage method: “complete”) was performed. The Spearman rank test was performed to analyze the coefficient of correlation between selected DEPs. Correlations with an *P*-value < .05 and *r* > .5 were considered significant. Gene ontology (GO) and Reactome pathway enrichment analyses were performed using the bioinformatics web tool PANTHER (<http://www.pantherdb.org/>).²² This tool was also used to perform overrepresentation test (*P* < .05) where all

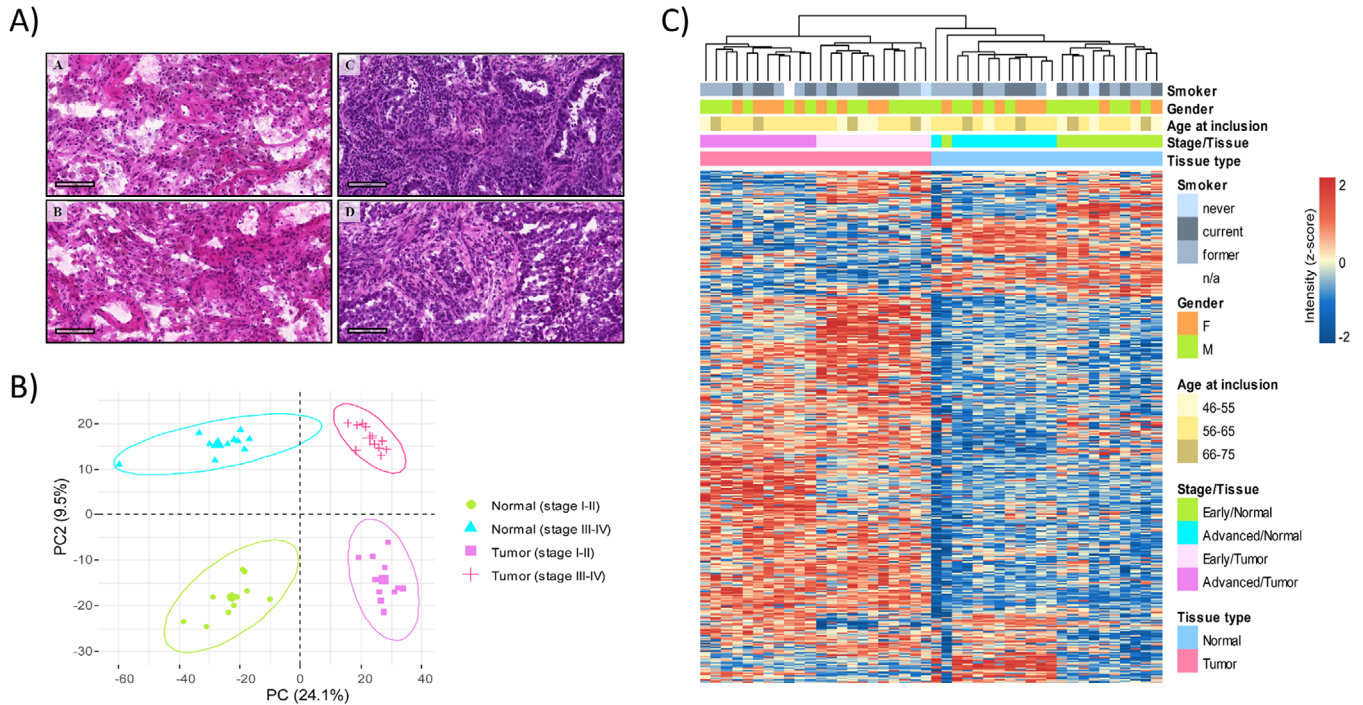


FIGURE 1 **A**, Representative H&E staining of tumor and normal adjacent tissue samples. It illustrates the representative tumor (right) and normal adjacent (left) tissue sections from early-stage ADC (A) and (C), and from advanced-stage ADC (B) and (D). **B**, Principal component analysis (PCA) of protein expression patterns of the 44 samples. The greatest variance (PC1_24.1%) is given by the differences between normal and tumor tissue and the second (PC2_9.5%) by differences between stages. **C**, Hierarchical clustering separated normal, early, and advanced ADC proteomes. Heat map and hierarchical clustering based on 1579 differentially expressed proteins (DEPs) from the ANOVA test. Heat map colors are based on the z-scored (\log_2) intensity values. Blue and red correspond to decreased and increased expression levels, respectively

identified proteins were used as the background list. STRING database was used to assess functional protein association networks (<https://string-db.org/>).

3 | RESULTS

3.1 | Lung ADC tissue proteomics

In this study, differences at the protein level between early-stage and advanced-stage lung ADC tissues were assessed. Malignant tumor samples and their nonmalignant adjacent tissue were also compared separately for early- and advanced-stage ADC. As shown in Figure 1A, the histology of the tissue samples was confirmed (Hematoxylin and Eosin [H&E] stained sections of tumor and adjacent normal lung tissue samples can be found in File F1 in the Supporting Information). Following enzymatic digestion, the extracted protein samples were individually analyzed on a Q-Exactive Plus Orbitrap coupled to peptide separation by LC.

Proteomic profiling was performed on matched malignant and normal tissues and a total of 4863 proteins were identified across all 22 tissue pairs (44 samples) (see Table S1). Using PCA, based on the protein expression of all pro-

teins quantified in all samples, a 2D scatterplot was generated to explore and distinguish all analyzed groups. In Figure 1B, the first versus the second principal component (PC) are represented. Importantly, the first PC (24.1% of explained variances) clearly separated control (“normal”) tissues (left) from tumor tissues (right). When focusing on the second PC (9.5% of explained variances), the data showed early-stage ADC and matched control tissues at the bottom of the plot, whereas advanced ADCs and matched controls are shown at the top. To detect overall changes across the four sample groups, an ANOVA test was performed and 1579 proteins result differentially expressed ($FDR < 1\%$) (see Table S2A). Based on the intensity of the DEPs, unsupervised hierarchical clustering of the 44 datasets confirmed that the normal, early, and advanced ADC proteomes were sufficiently distinct to be resolved from one another (Figure 1C) independently of other clinical characteristics of the patients (e.g., gender, age at inclusion, smoking status).

Our primary goal was to determine the differences in protein expression profiles between tumor and tissues with normal histology. Of the 4863 proteins, 2810 proteins (58%) were observed across all groups, whereas 703 proteins (14.5%) were shared among the advanced- and the early-stage ADC groups. A total of 300 and 172 proteins were

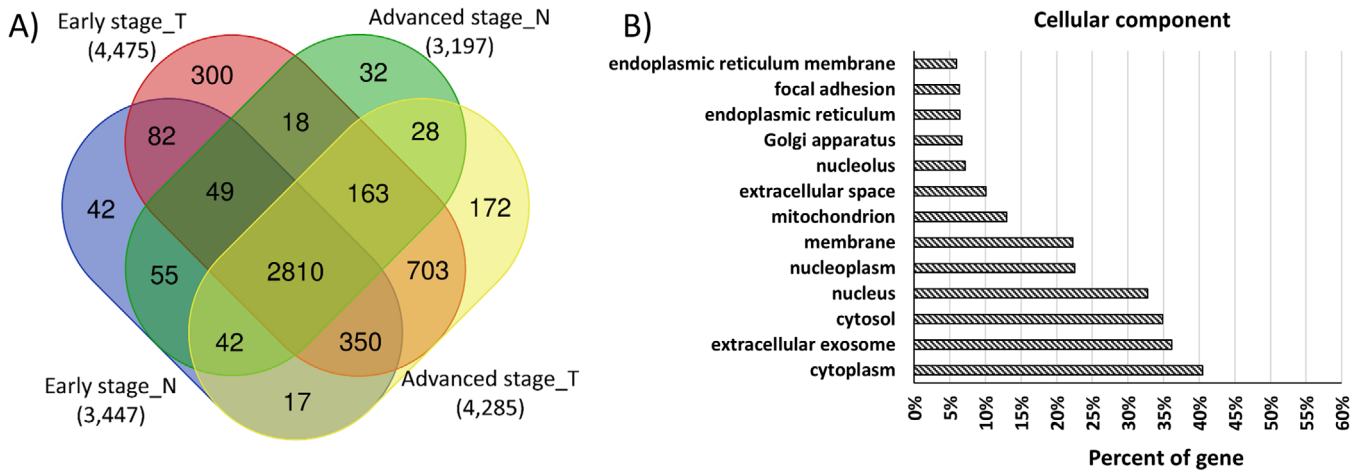


FIGURE 2 **A**, Venn diagrams showing the distribution of the identified protein groups across the sample classifications. T refers to tumor samples. N refers to adjacent normal tissue sample. **B**, Gene ontology (GO) annotation of identified proteins by cellular component

specific to early- and advanced-stage tumors, respectively (Figure 2A). When the number of proteins identified in the ADC tissues was compared to the matched control tissues, an increase in the complexity of the proteome in the tumor tissue was revealed. This observation is similar to the results obtained by Tenzer et al²³ (average protein number in normal tissue: 3322; average protein number in ADC: 4380). To obtain an overview of the cellular distribution of the identified proteins, these were classified according to the cellular component category of GO. Concerning cellular component, the majority of the proteins were assigned to the cytoplasm (40.5%), whereas 36.1% and 10% mapped to extracellular exosome and space, respectively. A total of 1677 (35%) proteins mapped to the cytosol, 2657 (55.2%) to nucleus and nucleoplasm, whereas 1070 (22.3%) to the membrane (Figure 2B). Overall, the distribution of the proteins was not biased toward a specific cell compartment.

3.2 | Differential protein expression between normal and tumor samples: Early stage

Comparison of the DEPs ($-2 \geq \log_2 FC \geq 2$; q -value $< .01$) between normal and tumor tissues showed that in early-stage tumor, 86 and 279 proteins were down- and upregulated, respectively (see Table S2B). The proteins with the greatest alteration in expression ($-4 \geq \log_2 FC \geq 4$) are depicted in Figure 3B as a heat map. The within-patient comparison between tumor and normal tissue is shown in Figure S1A for each patient with early-stage ADC.

The pathway analysis revealed that the upregulated proteins in tumor were associated with translation initiation and regulation of translation, such as nonsense-mediated decay and mRNA splicing (Table S3). Specifically, 12, 9, and

6 proteins were identified as ribosomal proteins, mRNA-splicing factors, and translation factors, respectively (Table S4).

A total of 224 proteins were exclusively quantified in the early-stage tumor tissues (in more than 70% of the samples), but not in the matched normal samples. Among these, 67 were identified in all the early-stage tumor samples (Table S5).

To assess potential pathways associated with early-stage ADC, these 236 proteins were further analyzed using the bioinformatics tool PANTHER. The GO-Slim biological process analysis revealed that these proteins are involved in mRNA splicing, DNA replication, and regulation of cell cycle (Table S6).

3.3 | Differential protein expression between normal and tumor samples: Advanced stage

Comparative analysis of the advanced-stage tumor tissues showed that 92 and 274 proteins were down- and upregulated, respectively, relative to the normal paired samples ($-2 \geq \log_2 FC \geq 2$; q -value $< .01$) (see Table S2C). Figure 4 shows a heat map performed with proteins that had the highest expression level alterations ($-4 \geq \log_2 FC \geq 4$). The within-patient comparison between tumor and normal tissue is shown in Figure S1B for each patient with advanced-stage ADC.

Pathway enrichment analysis of the 274 upregulated proteins revealed that a variety of cellular processes are overrepresented in advanced-stage lung ADC (Table S7). The upregulated proteins and enriched pathways are associated with mRNA splicing, translation, and regulation of translation. Specifically, seven proteins belong to the

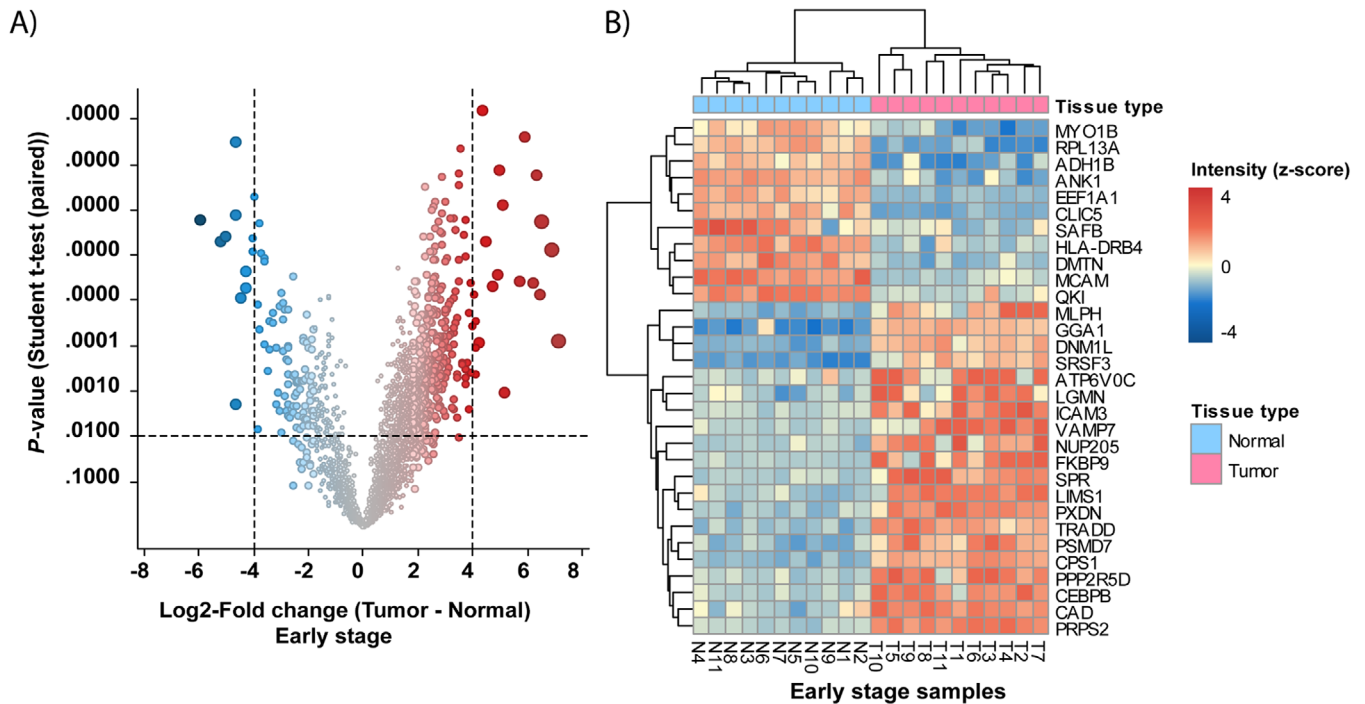


FIGURE 3 Differentially expressed proteins in early-stage ADC. **A**, Volcano plot of \log_2 -fold change (FC) versus P -value t -test. Points alter in size according to the magnitude of the fold change. **B**, Heat map generated by hierarchical clustering of the most altered proteins. The heat map shows a clear separation of adjacent normal and tumor tissues ($-4 \geq \log_2 FC \geq 4$, adj. $P < .01$). Blue and red correspond to decreased and increased expression levels, respectively

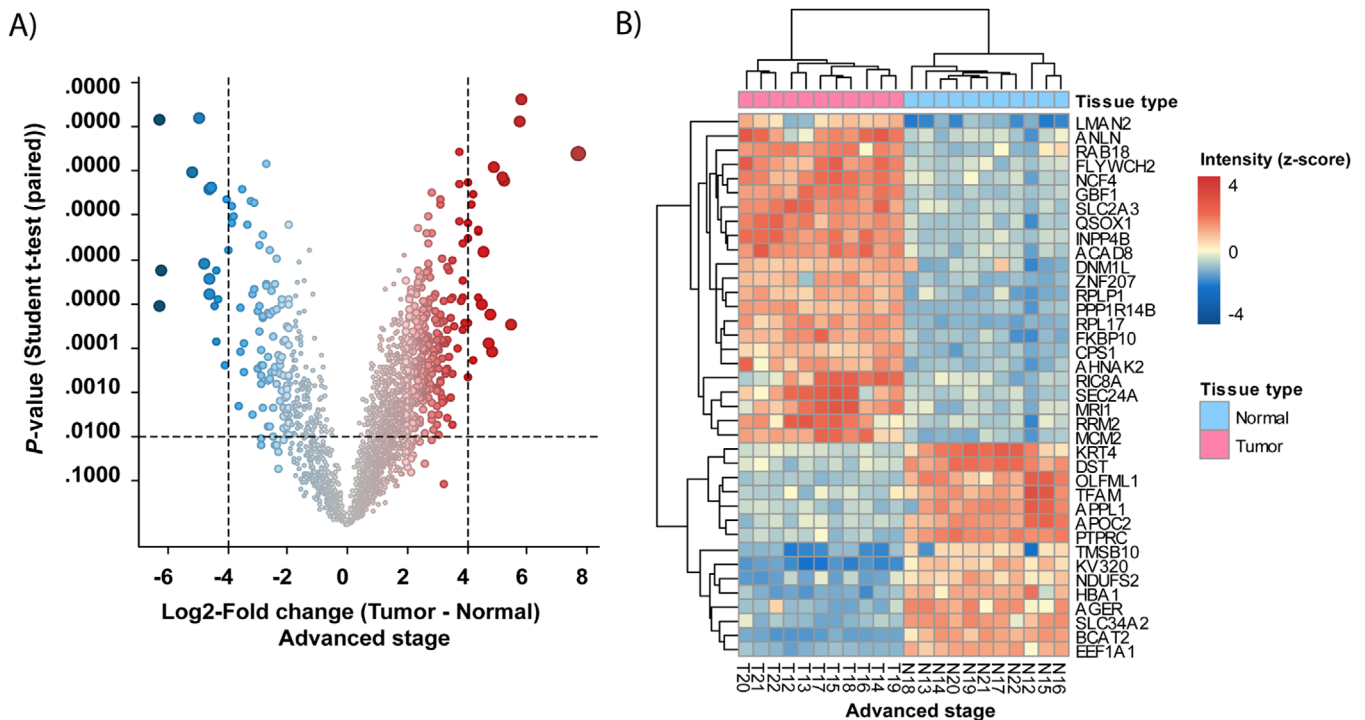


FIGURE 4 Comparison between normal and tumor tissue in advanced-stage ADC. **A**, Volcano plot of \log_2 -fold change (FC) versus P -value t -test. Points alter in size according to the magnitude of the fold change. **B**, Heat map generated by hierarchical clustering of the most altered proteins. The heat map shows a clear separation of adjacent normal and tumor tissues ($-4 \geq \log_2 FC \geq 4$, adj. $P < .01$). Blue and red correspond to decreased and increased expression levels, respectively

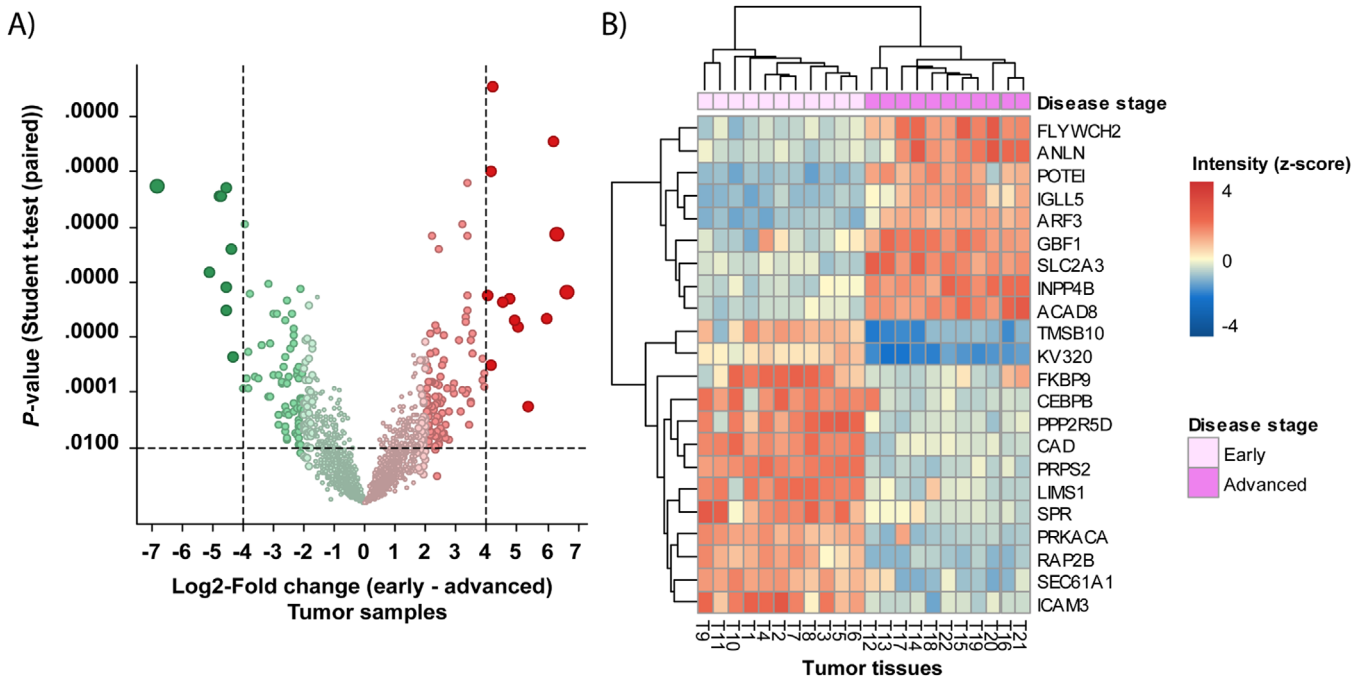


FIGURE 5 Comparison of early- and advanced-stages in tumor tissue. **A**, Volcano plot of \log_2 -fold change (FC) versus P -value t -test. Points alter in size according to the magnitude of the fold change. **B**, Heat map generated by hierarchical clustering of the most altered proteins. The heat map shows a clear separation of adjacent normal and tumor tissues ($-4 \geq \log_2 FC \geq 4$, adj. $P < .01$). Blue and red correspond to decreased and increased expression levels, respectively

family of mRNA splicing factors, seven ribosomal proteins were identified, and seven proteins are aminoacyl-tRNA synthetases (ARS) (Table S8). ARSs are important housekeeping proteins that play an essential role in protein synthesis. Accumulating evidence indicates that ARSs play an important role in cancer and it has been demonstrated that some ARSs show cancer-associated overexpression.²⁴⁻²⁶

3.4 | Proteins differentially-expressed between early- and advanced-stage ADC

To characterize early- and advanced-stage ADC, the proteins that were differentially expressed between the early and advanced tumor samples were determined. In total, 84 and 71 proteins were down- and upregulated, respectively, in advanced tumor tissue compared to early tumor tissue ($-2 \geq \log_2 FC \geq 2$; q -value $< .01$) (see Table S2D). The proteins with the highest altered expression ($-4 \geq \log_2 FC \geq 4$) are given in Table S2C and displayed as a heat map in Figure 5B.

Reactome pathway terms that are overrepresented in the 71 upregulated proteins were EPH-ephrin signaling (AP2A1, MYL9, and ACTB), signaling by Rho GTPases (MYL9, ACTB, GMIP, NCF4, ARHGEF1, and PIN1), and beta-catenin independent Wnt-signaling (AP2A1, PLCB2,

PSMD13, and PSMB5). All of which have been implicated in tumorigenesis (Table S9).

Moreover, pathways that are associated with the upregulated proteins are involved in tumorigenesis. These include the VEGFA-VEGFR2 pathway, insulin receptor signaling cascade, beta-catenin independent WNT signaling, signaling by Rho GTPases, and the RAF/MAP kinase cascade.

Reactome pathways associated with the downregulated proteins are involved in the extracellular matrix organization (ITGAX, FBN1, MMP2, ICAM3, COL6A2, and FGA), integrin cell surface interactions (ITGAX, FBN1, ICAM3, COL6A2, and FGA), degradation of the extracellular matrix (FBN1, MMP2, and COL6A2), and ECM proteoglycans (ITGAX and COL6A2) (Table S10).

3.5 | Early-stage ADC-specific proteins

At the protein level, distinct changes occur during tumor progression. Such changes range from altered expression and differential protein modification to changes in protein activity and altered localization. Detecting stage-specific changes in cancer proteomes may assist in identifying potential biomarkers that enable detection of the disease at an earlier stage.²⁷ Therefore, from the list of 67 proteins (Table S5) that were exclusively quantified in all early-stage ADC samples (but not in the matched normal samples),

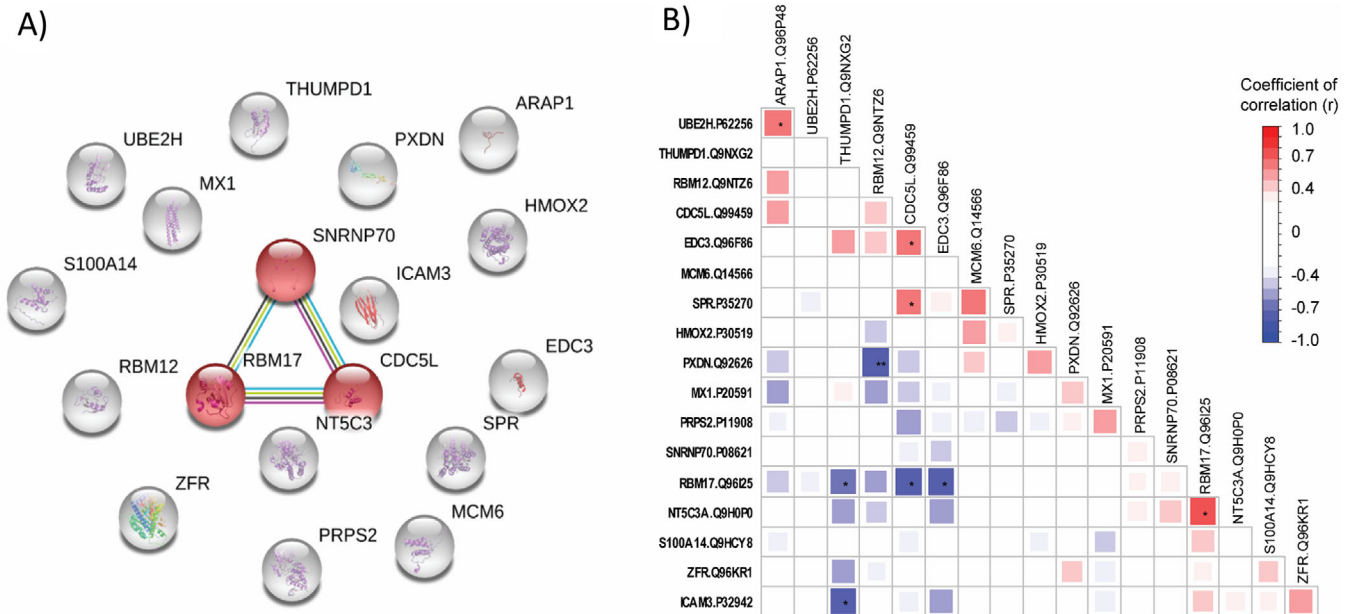


FIGURE 6 Protein-protein interaction and correlation for the 18 early-stage ADC-specific proteins. **A**, Protein network from STRING. Shown in red are the significant interactions (FDR < .05 with the highest confidence threshold). **B**, Spearman correlation. The color scale represents the strength of the correlation (r) (white to red, positive correlation; white to blue, negative correlation). * P < .05; ** P < .01

18 proteins were further assessed based on the differential expression between early- and advanced-stage ADC (Table 2). Out of 18, seven proteins were quantified in early but not in advanced ADC samples (ARAP1, ZFR, EDC3, HMOX2, NT5C3A, PRPS2, and ICAM3; referred as ON/OFF in Table 2) and 11 proteins were overexpressed in early-stage ADC (MCM6, SNRNP70, CDC5L, RBM12, RBM17, S100A14, THUMP1, MX1, UBE2H, PXDN, and SPR; adj. P -value < .01).

To analyze the associations among these 18 proteins (quantified in all early-stage samples), the STRING database was used to retrieve interacting genes/proteins. Following the STRING network analysis, only three proteins (all components of the spliceosome) showed a strong association with one another (Figure 6A). SNRNP70 (small nuclear ribonucleoprotein U1 subunit 70) associates with U1 snRNA and is essential for the 5' splice site selection. RBM17 (RNA-binding motif protein 17) is involved in the regulation of alternative splicing and is frequently overexpressed in various solid tumors.²⁸ CDC5L (cell division cycle 5 like) is a core component of the spliceosomal complex and essential for pre-mRNA splicing²⁹ and involved in DNA damage repair.³⁰ To date, several alterations in mRNA metabolism have been reported in lung cancer suggesting that mRNA metabolism-related proteins are involved in the pathology of the disease.^{31,32}

To further examine the relationship between the proteins, a Spearman correlation analysis was performed using the 11 values from early tumor stage. Only nine

significant correlations were observed among the 18 proteins. Positive correlations were apparent between RBM17 and NT5C3A; ARAP1 and UBE2H; CDC5L and EDC3; and CDC5L and SPR. Negative correlations were observed between RBM12 and PXDN; RBM17 and CDC5L; RBM17 and EDC3; THUMP1 and ICAM3; and RBM17 and THUMP1 (Figure 6B; Table S11). Interestingly, there were four significant correlations for the protein RBM17. Nevertheless, no evidence from the literature was found supporting an association between RBM17 and NT5C3A, and EDC3 and THUMP1. Taken together, the expression levels of the 18 proteins did show the same dynamics between the tumor stages, namely, upregulated in early-stage ADC and downregulated in advanced ADC tissues. These proteins, however, did not show any clear association with one another, neither with published data nor with our values. To enrich the number of related proteins, further research with a larger patient cohort is a necessity.

4 | DISCUSSION

In this study, the proteomes of early- and advanced-stage lung ADC plus normal adjacent tissue were generated. The identified proteins were described and the most DEPs between normal and tumor samples and between early- and advanced-stage tumor tissues were discussed. The generated data were also compared to currently available literature in the context of improving our understanding of the molecular basis of lung ADC.

TABLE 2 Top 18 potential early stage-specific proteins. These proteins were quantified in all tumor samples from early-stage ADC but not in their matched normal samples. The log₂-fold changes (FC) indicate that their intensities were higher in early ADC than in advanced ADC. ON/OFF: proteins quantified in early but not in advanced stage ADC samples. All proteins presented an adj. *P*-value < .01 (T-test_Early vs Advanced ADC)

Gene symbol	Protein name (UniProt accession)	Log ₂ FC (Early/Advanced ADC)	Known functions	Relation to cancer
ARAP1	ArfGAP With RhoGAP Domain, Ankyrin Repeat, and PH Domain 1 (Q96P48)	ON/OFF	Coordinates the membrane and actin remodeling involved in cell movement.	Prevents EGFR degradation. ^{88,89}
ZFR	Zinc finger RNA-binding protein (Q96KR1)	ON/OFF	Regulates alternative pre-mRNA splicing and plays an essential role in cell growth.	Potential therapeutic target in human pancreatic cancer. ⁹⁰ Involved in NSCLC tumor growth and metastasis. ⁹¹
EDC3	Enhancer Of MRNA decapping 3 (Q96F86)	ON/OFF	Component of mRNA decapping complex and involved in mRNA decay. ⁹³	–
HMOX2	Hem oxygenase 2 (P30519)	ON/OFF	Heme degradation to biliverdin, iron, and carbon monoxide, cytoprotective and anti-inflammatory function. ¹⁰⁷	May be associated with the prognosis of bladder cancer. ⁹²
NT5C3A	5'-Nucleotidase, cytosolic IIIA (Q9H0P0)	ON/OFF	Catalyzes the dephosphorylation of pyrimidine 5' monophosphates.	–
PRPS2	Phosphoribosyl pyrophosphate synthetase 2 (P11908)	ON/OFF	Plays a central role in the synthesis of pyrimidines and purines.	Promoted increased nucleotide biosynthesis in Myc-transformed cells. ⁴⁸
ICAM3	Intracellular adhesion molecule 3 (P32942)	ON/OFF	Constitutively and abundantly expressed by all leucocytes and may be the most important ligand for LFA-1 in the initiation of the immune response.	Promoted cancer cell migration and invasion. ¹⁰⁶ Induced cancer cell proliferation in vitro in lung cancer. ⁴⁴ Stimulated cancer cell migration/invasion via ICAM-3/Akt/CREB/MMP pathway in NSCLC cells. ⁴⁵
MCM6	Minichromosome maintenance complex component 6 (Q14566)	1.29	Essential component for DNA replication.	Overexpressed in NSCLC. Component of a 6-protein panel, which is a potential biomarker for the early detection of lung cancer in bronchial brushings. ¹⁰⁹
SNRNP70	Small nuclear ribonucleoprotein U1 subunit 70 (P08621)	1.60	Component of the spliceosome.	Its gene was found upregulated in lung ADC. ¹¹⁰
CDC5L	Cell division cycle 5 like (Q99459)	1.66	DNA-binding protein involved in cell cycle control, pre-mRNA splicing, and DNA damage response.	Implicated in colorectal cancer, ¹¹¹ prostate cancer, ¹¹² and hepatocellular carcinoma. ¹¹³
RBM12	RNA binding motif protein 12 (Q9NTZ6)	1.90	RNA-binding protein.	Upregulated in meibomian cell carcinoma. ¹¹⁴
RBM17	RNA binding motif protein 17 (Q96I25)	1.99	Component of the spliceosome complex.	Overexpressed in numerous carcinomas, including lung. ²⁸

(Continues)

TABLE 2 (Continued)

Gene symbol	Protein name (UniProt accession)	Log ₂ FC (Early/Advanced ADC)	Known functions	Relation to cancer
S100A14	S100 calcium-binding protein A14 (Q9HCY8)	2.01	Calcium-binding protein involved in cell proliferation and differentiation.	Implicated in tumorigenesis in various cancer types. ¹¹⁵⁻¹¹⁸ Overexpressed in lung ADC1; ¹¹⁹ its expression correlated with invasion of lung ADC cells. ¹²⁰
THUMPDI	THUMP domain containing 1 (Q9NXG2)	2.30	tRNA-binding adapter to mediate NAT10-dependent tRNA acetylation. ¹²¹	Overexpressed in breast cancer and promoted metastasis. ¹²²
MX1	MX dynamin like GTPase 1 (P20591)	2.31	Play a pivotal role in the type I interferon-mediated response against viral infections.	Potential bone metastasis biomarker in lung cancer. ¹²³
UBE2H	Ubiquitin conjugating enzyme E2 H (P62256)	3.35	E2 ubiquitin-conjugating enzyme.	Plays a role in HCC development. ^{124,125} MET-UBE2H fusion a novel resistance gene arrangement to EGFR-TKI in lung ADC. ¹²⁶
PXDN	Peroxidasin (Q92626)	3.54	Heme-containing peroxidase involved in the formation and stabilization of extracellular matrix.	Has been detected in several cancer types. ⁴³ Its overexpression is associated with poor prognosis in ovarian cancer. ¹²⁷
SPR	Sepiapterin reductase (P35270)	5.03	Catalyzes the last step of BH4 biosynthesis.	Over expression of SPR mRNA correlated with poor prognosis in neuroblastoma patients. ⁴¹

Over the past decade, considerable efforts have been made to discover potential protein biomarkers that can be used to detect and monitor the progression of lung cancer. Despite these efforts, however, lung cancer remains the leading cause of cancer-related mortality worldwide.³³ Thus, it is critical to obtain more knowledge on the molecular complexity of lung ADC.

MS-based proteomics enables the analysis of dynamic and complex systems in biology. Label-free proteomic analyses not only provide a list of identified proteins but also enable the quantitation of relative changes in protein expression levels between sets of samples. Both prognostic and predictive biomarkers for lung cancer found in tissue, cells, blood, or other body fluids have been discovered using MS-based proteomics approaches (reviewed by Cheung and Juan⁹). The application of proteomic analyses of paired tumor and control tissue can aid in the investigation of pathological processes in lung ADC. In this study, a label-free proteomics workflow was applied. The protocol required minimal sample manipulation and was versatile and cost-effective.

During the analysis of the proteomic profiles of the paired tumor and normal lung tissues, an observation

was made whereby the number of identified proteins was higher in the cancer tissues compared to the matched controls (average protein number in normal tissue: 3272; average protein number in ADC: 4336).

4.1 | DEPs in early- and advanced-stage ADC

Many of the DEPs between normal and tumor samples (early stage) have been previously implicated in tumorigenesis in the literature. The RNA-binding protein QKI is a key regulator of alternative splicing in lung cancer and has been frequently reported as downregulated in lung cancer. Downregulation is associated with poor prognosis.³⁴ SAFB (scaffold attachment factor B) belongs to the nuclear matrix family of proteins and low-protein expression is significantly associated with worse overall survival in breast cancer patients who did not receive adjuvant therapy.³⁵ A decreased level of the protein ANK1 (ankyrin 1) that is known to regulate cell shape and membrane integrity has been observed in lung ADC.³⁶ Ion channels are involved in diverse biological functions and

it is known that dysregulated expression of such proteins contributes to tumor progression.³⁷ Recently, the gene expression profile of 37 ion channels was analyzed in lung ADC. Several ion channels including CLIC3 (chloride intracellular channel 3) were downregulated.³⁸

BH4 (tetrahydrobiopterin) synthesis promotes both endothelial cell proliferation, migration, and tube formation in vitro and angiogenesis in tumor xenografts.³⁹ Moreover, BH4 induces A549 cell proliferation and migration via the activation of Akt and p70^{S6K} signaling.⁴⁰ In tumorigenesis, relatively little is known about the role of SPR (sepiapterin reductase) that catalyzes the last step of BH4 biosynthesis. Recently, Lange et al⁴¹ reported an oncogenic role for SPR in neuroblastoma and found that overexpression of SPR mRNA correlates with poor prognosis in patients. DNMI1 (dynamitin 1-like protein) is essential for normal mitochondrial function and is upregulated in several cancer types including lung cancer.⁴² PXDN (peroxidase) is involved in the formation and stabilization of the ECM and has been detected in several types of cancer.⁴³ ICAM3 (intracellular adhesion molecule 3) has been shown to induce cancer cell proliferation in vitro in lung cancer⁴⁴ and promote cancer cell migration and invasion.⁴⁵ SRSF3 (serine arginine-rich splicing factor 3) is a well-known RNA processing protein that is overexpressed in several cancer types and involved in tumor maintenance.⁴⁶ CPS1 (carbamoyl-phosphate synthase 1) is a multi-domain mitochondrial enzyme that is involved in arginine and pyrimidine metabolism and was shown to be statistically significantly associated with poor overall survival in stage I lung ADC.⁴⁷ Cancer cells have the ability to alter cellular processes to sustain an enhanced metabolism for increased cell growth and proliferation. Recently, it has been reported that PRPS2 (phosphoribosyl pyrophosphate synthetase 2), a protein that plays a central role in the synthesis of pyrimidines and purines, promoted increased nucleotide biosynthesis in Myc-transformed cells.⁴⁸ PAIP1 (poly(A)-binding protein-interacting protein 1) was detected only in tumor tissue and overexpression of PAIP1 in vitro stimulates translation.⁴⁹

Among the dysregulated protein between normal and tumor samples (advanced stage), INPPB4 (type II inositol 3,4-bisphosphate 4-phosphatase) has been previously identified as a tumor suppressor and expression of this protein is reduced in several types of cancers including breast, ovarian, and prostate.⁵⁰⁻⁵² A recent report, however, indicated that INPPB4 promotes an oncogenic signaling pathway in breast cancer.⁵³

QSOX1 (quiescin sulphydryl oxidase 1) has an emerging role in cancer and was shown to be overexpressed in several malignancies including breast, pancreas, and prostate cancer.^{54,55} A general consensus is emerging that QSOX1 overexpression is important during tumor cell inva-

sion, facilitating tumor cell migration at the tumor-stroma interface.⁵⁶ Recently, it was reported that LMAN2 (vesicular integral-membrane protein VIP36) is overexpressed in gastric cancer.⁵⁷

4.2 | Early versus advanced ADC

Some of the upregulated proteins in early-stage ADC were ribosomal proteins, mRNA-splicing factors, and translation factors. Emerging evidence suggests that ribosomal proteins not only play essential roles in protein synthesis, but are also involved in cancer tumorigenesis.⁵⁸⁻⁶⁰ Recently, it was demonstrated that RPS15A (ribosomal protein S15A) expression is increased in lung ADC tissue and knockdown of RPS15A inhibited cancer cell growth and induced apoptosis.⁶¹ It has been suggested that RPS6 (ribosomal protein 6) is overexpressed in NSCLC and downregulation thereof inhibits cell growth.⁶² It is well known that aberrant mRNA splicing contributes to cancer progression and the expression of splicing factors are altered in tumor tissues.⁶³⁻⁶⁶ Gout et al⁶⁷ suggested that global deregulation of pre-mRNA splicing factors occurs during lung tumorigenesis. These researchers demonstrated that SRSF1 and SRSF2 (serine and arginine-rich splicing factor 1 and 2) and SRPK1 and SRPK2 SRSF protein-specific kinases are upregulated in NSCLC. In our study, SRSF7 and SRSF2 were statistically significantly up- and downregulated in advanced ADC, respectively (q -value < .01), but did not meet the established criteria for FC (\log_2 FC = 1.126; \log_2 FC = -1.618, respectively). On the other hand, a prognostic mRNA splicing signature was identified by Gout et al⁶⁷ in lung ADC and splicing networks were revealed. Together, these could reveal novel cancer drivers and provide new insight in lung ADC etiology.⁶⁸ Translational regulation is a critical process for maintaining cellular homeostasis and allowing rapid cell adaptation under stress. Therefore, it is not surprising that dysregulated translation plays an important role in tumorigenesis.⁶⁹ Expressions of specific subunits of EIF3 are altered in a variety of human tumors. Elevated expression of EIF3A was observed in lung cancer⁷⁰ and overexpression of the eucaryotic translation initiation factor 4E and 4H in lung cancer has also been reported.^{71,72} Moreover, phase II clinical trials of an EIF4E antisense oligonucleotide (ASO) combined with carboplatin and paclitaxel for NSCLC are ongoing (NCT01234038).

Several of the upregulated proteins in advanced ADC samples have been previously reported in the literature as involved in tumor progression. Serum levels of POTE (POTE ankyrin domain family member I), a paralog of POTEI (POTE ankyrin domain family member I), in NSCLC patients are associated with TNM stage (tumor

extension, nodal status, and metastatic spread incorporated into the staging system).⁷³ ARF3 (ADP-ribosylation factor 3) belongs to the human ADP-ribosylation factor gene family and is involved in vesicular trafficking. The actin-binding protein ANLN (actin-binding protein anillin) is a ubiquitously expressed protein required for cytokinesis. Upregulation of ANLN expression is frequently observed during cancer development, growth, and progression.^{74,75} Moreover, it has been reported that nuclear ANLN protein expression in lung cancer tissue is significantly correlated with poor survival.⁷⁶ Aberrant expression of SLC2A3 (solute carrier family 2, facilitated glucose transporter member 3) has been reported in gastric, testicular, ovarian, and NSCLC.^{77,78} Furthermore, it has been shown that SLC2A3 induces tumor cell proliferation in NSCLC.⁷⁹

On the other hand, extracellular matrix organization (ECM) was associated with proteins downregulated in advanced ADC. It is well-known that cancer development and progression is associated with ECM. The ECM is a highly dynamic structure and a major component of the microenvironment. Abnormal ECM dynamic leads to dysregulated cell proliferation and migration.^{80,81} Collagen is the most abundant constituent of the ECM and increased or decreased expression of collagen can contribute to increased malignancy.⁸²⁻⁸⁴ CEACAM6 overexpression was previously reported in various types of cancer including NSCLC.⁸⁵ Dysregulated overexpression of CEACAM6 is oncogenic and associated with an invasive tumor phenotype.⁸⁶

The most abundant protein observed in early-stage tumor tissues was FKBP9 (peptidyl-prolyl cis-trans isomerase FKBP9) (upregulated in early-stage tumor tissues). This protein belongs to the family of peptidyl-prolyl isomerases (PPIase) that catalyze peptidyl-prolyl cis-trans isomerization and function as molecular chaperones that play a crucial role in tumorigenesis. PPIases mediate conformational modifications in proteins that modulate signaling pathways and are overexpressed in a variety of tumors.⁸⁷ Development of isoenzyme-specific inhibitors has been in the focus of recent biomedical research.

4.3 | Early-stage ADC-specific proteins

The detection of proteomic changes that occur during tumor progression may aid in identifying potential stage-specific markers for diagnosis. The prognosis for lung cancer patients is strongly related to the stage of the disease at the time of diagnosis. Seven of the 18 early stage-specific proteins were identified only in the early stage ADC samples (referred as ON/OFF in Table 2). ARAP1 (ArfGAP with RhoGAP domain, ankyrin repeat,

and PH domain 1) prevents EGFR degradation^{88,89} and thus may increase the oncogenic capabilities of the cells. ZFR (zinc finger RNA-binding protein) is involved in the regulation of alternative pre-mRNA splicing and plays an essential role in cell growth and maybe a potent therapeutic target in human pancreatic cancer.⁹⁰ In a recent study, it was demonstrated that ZFR is involved in NSCLC tumor growth and metastasis.⁹¹ Among the 18 selected proteins, 11 were also observed in the advanced-stage tumor samples (Table 2). These were downregulated in advanced-stage ADC suggesting that expression thereof may be early stage specific.

Several of the proteins quantified exclusively the early-stage tumor tissues have been implicated in cancer. HMOX2 (heme oxygenase 2) may be associated with the prognosis of bladder cancer.⁹² ZFR has been reported to play an important role in DNA binding and plays an essential role in cell growth and maybe a potent therapeutic target in human pancreatic cancer.⁹⁰

Although several of the selected early-stage ADC-specific proteins have been reported to play a role in tumorigenesis in various cancer types (Table 2), EDC3 and NT5C3A have not been implicated in lung cancer. EDC3 (enhancer of mRNA decapping 3) is a component of the mRNA decapping complex and important for mRNA stability and decay.⁹³ Removal of the 5' end cap structure from mRNAs is a crucial control step in the cytoplasmic degradation of mRNAs, and thus an essential process in posttranscriptional regulation of gene expression.^{94,95} Alterations in the protein expression level of specific mRNA decapping factors may lead to a deregulated mRNA decay pathway and potentially contribute to tumorigenesis.^{96,97} NT5C3A (5'-nucleotidase, cytosolic IIIA) is a member of the 5'-nucleotidase family and participates in nucleotide homeostasis by catalyzing the dephosphorylation of pyrimidine monophosphates.⁹⁸ It has been demonstrated that NT5C3A plays a critical role in the metabolism of, and resistance to, chemotherapeutic nucleoside analogues such as gemcitabine and cytosine arabinoside.⁹⁹ Recently, it has been shown that NT5C3A acts as a negative regulator of the inflammatory cytokine response.¹⁰⁰ Aberrations in the cytokine response pathways can alter gene expression subsequently leading to tumor progression.¹⁰¹

These potential stage-specific proteins require further additional investigation across a larger patient cohort.

4.4 | Proteomics studies with lung ADC samples

The survival rate of lung cancer patients strongly correlates with tumor stage. Therefore, improving diagnostic

strategies for early tumor detection may lead to an increase in patient survival. An approach using iTRAQ labeling recently identified 133 protein candidates from paired lung ADC with differing degrees of lymph node involvement.¹⁰² Six potential biomarkers that were overexpressed in ADC tissue comparing to adjacent normal tissues were further validated (ERO1L, NARS, PABPC4, RCC1, RPS25, and TARS). In addition, ERO1L and NARS were positively associated with lymph node metastasis.¹⁰² Employing a gel-free proteomic approach, Kawamura et al identified 81 proteins that were associated with stage IA and IIIA lung ADC from FFPE tissues. Napsin-A (NAPSA) and anterior gradient protein 2 homolog (AGR2) were identified as potential stage-specific candidates for stage IA and stage IIIA lung ADC.¹⁰³ In a recent study, zyxin (ZYG)—a novel potential early diagnostic biomarker—was identified from plasma by LC-SRM.¹⁰⁴

5 | CONCLUSIONS

We demonstrated that the proteomic workflow used here enabled a clear distinction between lung ADC and matched normal tissue samples and also between early- and advanced-stage tumor specimens. Our large-scale, label-free proteomic dataset of histologically well-classified lung ADC may provide a deeper insight into the molecular mechanisms underlying lung ADC progression. As expected, the complexity of the proteome from the tumor was higher than the normal tissue proteome. Thirty-three and 39 DEPs were identified in early- and advanced-stage ADC, respectively (adj. *P*-value < .01, FC ≥ 4). Although several of these proteins have been indicated in tumorigenesis and progression, none had been previously reported for lung ADC. Based on the biological functions of these proteins, the results revealed that the most enriched pathways are involved in mRNA metabolism. Furthermore, 18 potential early stage-specific proteins were identified that may be useful as predictive markers for lung ADC. To validate the findings of this study, a larger sample size/patient cohort and/or orthogonal methods are imperative.

ACKNOWLEDGMENTS

This study was supported by the Berta Kamprad Foundation, ThermoFisher Scientific, Global, and Liconic Biobanking, and was also supported by grants from the [National Research Foundation of Korea](#), funded by the Korean government (2015K1A1A2028365 and 2016K2A9A1A03904900) and Brain Korea 21 Plus Project, Republic of Korea, as well as the NIH/NCI International Cancer Proteogenome Consortium. AMS was supported

by the KNN121510 and NVKP_16-1-2016-0042 grants by the National Research, Development and Innovation Office of Hungary and Bolyai Research Scholarship of the Hungarian Academy of Sciences. BD acknowledges, funding from the Hungarian National Research, Development and Innovation Office (KH130356, K129065). BD and VL were also supported by the Austrian Science Fund (FWF I3522, FWF I3977 and I4677). VL is a recipient of Janos Bolyai Research Scholarship of the Hungarian Academy of Sciences and the UNKP-19-4 New National Excellence Program of the Ministry for Innovation and Technology.

CONFLICT OF INTEREST

The authors declare no conflict of interest.

DATA AVAILABILITY STATEMENT

The mass spectrometry proteomics data have been deposited to the ProteomeXchange Consortium via the PRIDE¹⁰⁵ partner repository with the dataset identifier PXD019259.

ORCID

Indira Pla  <https://orcid.org/0000-0002-0839-7829>

REFERENCES

- Saito S, Espinoza-Mercado F, Liu H, Sata N, Cui X, Soukiasian HJ. Current status of research and treatment for non-small cell lung cancer in never-smoking females. *Cancer Biol Ther.* 2017;18:359-368.
- Dela Cruz CS, Tanoue LT, Matthay RA. Lung cancer: epidemiology, etiology, and prevention. *Clin Chest Med.* 2011;32:605-644.
- Lawrence MS, Stojanov P, Polak P, et al. Mutational heterogeneity in cancer and the search for new cancer-associated genes. *Nature.* 2013;499:214-218.
- The Cancer Genome Atlas Research Network. Comprehensive molecular profiling of lung adenocarcinoma. *Nature.* 2014;511:543-550.
- Paez JG, Jänne PA, Lee JC, et al. EGFR mutations in lung cancer: correlation with clinical response to gefitinib therapy. *Science.* 2004;304:1497-1500.
- Bergethson K, Shaw AT, Ignatius Ou S-H, et al. ROS1 rearrangements define a unique molecular class of lung cancers. *J Clin Oncol.* 2012;30:863-870.
- Travis WD, Brambilla E, Riely GJ. New pathologic classification of lung cancer: relevance for clinical practice and clinical trials. *J Clin Oncol.* 2013;31:992-1001.
- Siegel RL, Miller KD, Jemal A. Cancer statistics, 2015. *CA Cancer J Clin.* 2015;65:5-29.
- Cheung CHY, Juan HF. Quantitative proteomics in lung cancer. *J Biomed Sci.* 2017;24:37.
- Wang H, Shi T, Qian W-J, et al. The clinical impact of recent advances in LC-MS for cancer biomarker discovery and verification. *Expert Rev Proteomics.* 2016;13:99-114.

11. Fujii K, Nakamura H, Nishimura T. Recent mass spectrometry-based proteomics for biomarker discovery in lung cancer, COPD, and asthma. *Expert Rev Proteomics*. 2017;14:373-386.
12. Mason JT. Proteomic analysis of FFPE tissue: barriers to clinical impact. *Expert Rev Proteomics*. 2016;13:801-803.
13. Crutchfield CA, Thomas SN, Sokoll LJ, Chan DW. Advances in mass spectrometry-based clinical biomarker discovery. *Clin Proteomics*. 2016;13:1.
14. Welinder C, Pawłowski K, Sugihara Y, et al. A protein deep sequencing evaluation of metastatic melanoma tissues. *PLoS One*. 2015;10:e0123661.
15. Kessner D, Chambers M, Burke R, Agus D, Mallick P. ProteoWizard: open source software for rapid proteomics tools development. *Bioinformatics*. 2008;24:2534-2536.
16. Sturm M, Bertsch A, Gröpl C, et al. OpenMS – an open-source software framework for mass spectrometry. *BMC Bioinformatics*. 2008;9:163.
17. Tyanova S, Temu T, Sinitcyn P, et al. The Perseus computational platform for comprehensive analysis of (prote)omics data. *Nat Methods*. 2016;13:731-740.
18. R Core Team. R: a language and environment for statistical computing. Vienna, Austria: R Foundation for Statistical Computing; 2016.
19. RStudio Team. RStudio: integrated development for R. Boston, MA: RStudio; 2016.
20. Pearson KL. On lines and planes of closest fit to systems of points in space. *Philos Mag Ser*. 1901;6(2):559-572.
21. Hotelling H. Analysis of a complex of statistical variables into principal components. *J Educ Psychol*. 1933;24:417-441.
22. Mi H, Huang X, Muruganujan A, et al. PANTHER version 11: expanded annotation data from Gene Ontology and Reactome pathways, and data analysis tool enhancements. *Nucleic Acids Res*. 2017;45:D183-D189.
23. Tenzer S, Leidinger P, Backes C, et al. Integrated quantitative proteomic and transcriptomic analysis of lung tumor and control tissue: a lung cancer showcase. *Oncotarget*. 2016;7:14857-14870.
24. Kim D, Kwon NH, Kim S. Association of aminoacyl-tRNA synthetases with cancer. *Top Curr Chem*. 2014;344:207-245.
25. Shin S-H, Kim Ho-S, Jung S-H, Xu H-D, Jeong Y-B, Chung Y-J. Implication of leucyl-tRNA synthetase 1 (LARS1) overexpression in growth and migration of lung cancer cells detected by siRNA targeted knock-down analysis. *Exp Mol Med*. 2008;40:229-236.
26. Vellaichamy A, Sreekumar A, Strahler JR, et al. Proteomic interrogation of androgen action in prostate cancer cells reveals roles of aminoacyl tRNA synthetases. *PLoS One*. 2009;4:e7075.
27. Hanash S, Taguchi A. Application of proteomics to cancer early detection. *Cancer J*. 2011;17:423-428.
28. Sampath J, Long PR, Shepard RL, et al. Human SPF45, a splicing factor, has limited expression in normal tissues, is overexpressed in many tumors, and can confer a multidrug-resistant phenotype to cells. *Am J Pathol*. 2003;163:1781-1790.
29. Ajuh P, Kuster Bernhard, Panov Kostya, et al. Functional analysis of the human CDC5L complex and identification of its components by mass spectrometry. *EMBO J*. 2000;19:6569-6581.
30. Mu R, Wang Y-B, Wu M, et al. Depletion of pre-mRNA splicing factor Cdc5L inhibits mitotic progression and triggers mitotic catastrophe. *Cell Death Dis*. 2017;5:e1151-e1151.
31. Valles I, Pajares MJ, Segura V, et al. Identification of novel deregulated RNA metabolism-related genes in non-small cell lung cancer. *PLoS One*. 2012;7:e42086.
32. Li L, Wei Y, To C, et al. Integrated Omic analysis of lung cancer reveals metabolism proteome signatures with prognostic impact. *Nat Commun*. 2014;5:5469.
33. Cheng T-YD, Cramb SM, Baade PD, et al. The international epidemiology of lung cancer: latest trends, disparities, and tumor characteristics. *J Thorac Oncol*. 2016;11:1653-1671.
34. Zong F-Y, Fu X, Wei W-J, et al. The RNA-binding protein QKI suppresses cancer-associated aberrant splicing. *PLoS Genet*. 2014;10:e1004289.
35. Hammerich-Hille S, Bardout VJ, Hilsenbeck SG, Osborne CK, Oesterreich S. Low SAFB levels are associated with worse outcome in breast cancer patients. *Breast Cancer Res Treat*. 2010;121:503-509.
36. Fahrman JF, Grapov D, Phinney BS, et al. Proteomic profiling of lung adenocarcinoma indicates heightened DNA repair, antioxidant mechanisms and identifies LASP1 as a potential negative predictor of survival. *Clin Proteomics*. 2016;13:31.
37. Pedersen SF, Stock C. Ion channels and transporters in cancer: pathophysiology, regulation, and clinical potential. *Cancer Res*. 2013;73:1658-1661.
38. Ko J-H, Gu W, Lim I, et al. Ion channel gene expression in lung adenocarcinoma: potential role in prognosis and diagnosis. *PLoS One*. 2014;9:e86569.
39. Chen L, Zeng X, Wang J, et al. Roles of tetrahydrobiopterin in promoting tumor angiogenesis. *Am J Pathol*. 2010;177:2671-2680.
40. Cho Y-R, Choi SW, Seo D-W. Sepiapterin regulates cell proliferation and migration: its association with integrin $\alpha 3\beta 1$ and p53 in human lung cancer cells. *Genes Genomics*. 2011;33:577-582.
41. Lange I, Geerts D, Feith DJ, Mocz G, Koster J, Bachmann AS. Novel interaction of ornithine decarboxylase with sepiapterin reductase regulates neuroblastoma cell proliferation. *J Mol Biol*. 2014;426:332-346.
42. Rehman J, Zhang HJ, Toth PT, et al. Inhibition of mitochondrial fission prevents cell cycle progression in lung cancer. *FASEB J*. 2012;26:2175-2186.
43. Jayachandran A, Prithviraj P, Lo Pu-H, et al. Identifying and targeting determinants of melanoma cellular invasion. *Oncotarget*. 2016;7:41186-41202.
44. KIM Y, Kim M, Lim J, Lee M, Kim J, Yoo Y. ICAM-3-induced cancer cell proliferation through the PI3K/Akt pathway. *Cancer Lett*. 2006;239:103-110.
45. Park JK, Park SH, So K, Bae IH, Yoo Y Do, Um H/D, et al. ICAM-3 enhances the migratory and invasive potential of human non-small cell lung cancer cells by inducing MMP-2 and MMP-9 via Akt and CREB. *Int J Oncol*. 2010;36(1):181-192. https://doi.org/10.3892/ijo_00000489.
46. Shilo A, Siegfried Z, Karni R. The role of splicing factors in deregulation of alternative splicing during oncogenesis and tumor progression. *Mol Cell Oncol*. 2015;2:e970955.
47. Çelikaş M, Tanaka I, Chandra Tripathi S, et al. Role of CPS1 in cell growth, metabolism, and prognosis in LKB1-inactivated lung adenocarcinoma. *J Natl Cancer Inst*. 2017;109:djw231.
48. Cunningham JT, Moreno MV, Lodi A, Ronen SM, Ruggero D. Protein and nucleotide biosynthesis are coupled by

- a single rate-limiting enzyme, PRPS2, to drive cancer. *Cell*. 2014;157:1088-1103.
49. Sonenberg N, Craig AWB, Haghghat A, Yu ATK. Interaction of polyadenylate-binding protein with the eIF4G homologue PAIP enhances translation. *Nature*. 1998;392:520-523.
 50. Kofuji S, Kimura H, Nakanishi H, et al. INPP4B is a PtdIns(3,4,5)P3 phosphatase that can act as a tumor suppressor. *Cancer Discov*. 2015;5:730-739.
 51. Hodgson MC, Shao L-J, Frolov A, et al. Decreased expression and androgen regulation of the tumor suppressor gene INPP4B in prostate cancer. *Cancer Res*. 2011;71:572-582.
 52. Gewinner C, Wang ZC, Richardson A, et al. Evidence that inositol polyphosphate 4-phosphatase type II is a tumor suppressor that inhibits PI3K signaling. *Cancer Cell*. 2009;16:115-125.
 53. Gasser JA, Inuzuka H, Lau AW, Wei W, Beroukhim R, Toker A. SGK3 mediates INPP4B-dependent PI3K signaling in breast cancer. *Mol Cell*. 2014;56:595-607.
 54. Antwi K, Hostetter G, Demeure MJ, et al. Analysis of the plasma peptidome from pancreas cancer patients connects a peptide in plasma to overexpression of the parent protein in tumors. *J Proteome Res*. 2009;8:4722-4731.
 55. Katchman BA, Ocal IT, Cunliffe HE, et al. Expression of quiescin sulfhydryl oxidase 1 is associated with a highly invasive phenotype and correlates with a poor prognosis in Luminal B breast cancer. *Breast Cancer Res*. 2013;15:R28.
 56. Lake DF, Faigel DO. The emerging role of QSOX1 in cancer. *Antioxid Redox Signal*. 2014;21:485-496.
 57. Marimuthu A, Subbannayya Y, Sahasrabuddhe NA, et al. SILAC-based quantitative proteomic analysis of gastric cancer secretome. *Proteomics Clin Appl*. 2013;7:355-366.
 58. Zhou X, Liao W-J, Liao J-M, Liao P, Lu H. Ribosomal proteins: functions beyond the ribosome. *J Mol Cell Biol*. 2015;7:92-104.
 59. Takada H, Kurisaki A. Emerging roles of nucleolar and ribosomal proteins in cancer, development, and aging. *Cell Mol Life Sci*. 2015;72:4015-4025.
 60. Wang W, Nag S, Zhang Xu, et al. Ribosomal proteins and human diseases: pathogenesis, molecular mechanisms, and therapeutic implications. *Med Res Rev*. 2015;35:225-285.
 61. Zhang Y, Zhang G, Li X, Li B, Zhang X. The effect of ribosomal protein S15a in lung adenocarcinoma. *PeerJ*. 2016;4:e1792.
 62. Chen B, Zhang W, Gao J, et al. Downregulation of ribosomal protein S6 inhibits the growth of non-small cell lung cancer by inducing cell cycle arrest, rather than apoptosis. *Cancer Lett*. 2014;354:378-389.
 63. Kelemen O, Convertini P, Zhang Z, et al. Function of alternative splicing. *Gene*. 2013;514:1-30.
 64. Stamm S. Alternative splicing and human disease. *eLS*. 2017. <https://doi.org/10.1002/9780470015902.a0021435.pub2>
 65. Sveen A, Kilpinen S, Ruusulehto A, Lothe RA, Skotheim RI. Aberrant RNA splicing in cancer; expression changes and driver mutations of splicing factor genes. *Oncogene*. 2016;35:2413-2427.
 66. Dvinge H, Kim E, Abdel-Wahab O, Bradley RK. RNA splicing factors as oncoproteins and tumour suppressors. *Nat Rev Cancer*. 2016;16:413-430.
 67. Gout S, Brambilla E, Boudria A, et al. Abnormal expression of the pre-mRNA splicing regulators SRSF1, SRSF2, SRPK1 and SRPK2 in non small cell lung carcinoma. *PLoS One*. 2012;7:e46539.
 68. Li Y, Sun N, Lu Z, et al. Prognostic alternative mRNA splicing signature in non-small cell lung cancer. *Cancer Lett*. 2017;393:40-51.
 69. Sharma DK, Bressler K, Patel H, Balasingam N, Thakor N. Role of eukaryotic initiation factors during cellular stress and cancer progression. *J Nucleic Acids*. 2016;2016:1-19.
 70. Pincheira R, Chen Q, Zhang JT. Identification of a 170-kDa protein over-expressed in lung cancers. *Br J Cancer*. 2001;84:1520-1527.
 71. Li Y, Fan S, Koo J, et al. Elevated expression of eukaryotic translation initiation factor 4E is associated with proliferation, invasion and acquired resistance to erlotinib in lung cancer. *Cancer Biol Ther*. 2012;13:272-280.
 72. Bauer K, Brass N, Diesinger I, Kayser K, Grässer FA, Meese E. Overexpression of the eukaryotic translation initiation factor 4G (eIF4G-1) in squamous cell lung carcinoma. *Int J cancer*. 2002;98:181-185.
 73. Wang Q, Li X, Ren S, et al. Serum levels of the cancer-testis antigen POTEE and its clinical significance in non-small-cell lung cancer. *PLoS One*. 2015;10:e0122792.
 74. Hall PA, Todd CB, Hyland PL, et al. The septin-binding protein anillin is overexpressed in diverse human tumors. *Clin Cancer Res*. 2005;11:6780-6786.
 75. Olakowski M, Tyszkiewicz T, Jarzab M, et al. NBL1 and anillin (ANLN) genes over-expression in pancreatic carcinoma. *Folia Histochem Cytobiol*. 2009;47:249-255.
 76. Suzuki C, Daigo Y, Ishikawa N, et al. ANLN plays a critical role in human lung carcinogenesis through the activation of RHOA and by involvement in the phosphoinositide 3-kinase/AKT pathway. *Cancer Res*. 2005;65:11314-11325.
 77. Younes M, Lechago LV, Somoano JR, Mosharaf M, Lechago J. Immunohistochemical detection of Glut3 in human tumors and normal tissues. *Anticancer Res*. 1997;17:2747-2750.
 78. Tsukioka M, Matsumoto Y, Noriyuki M, et al. Expression of glucose transporters in epithelial ovarian carcinoma: correlation with clinical characteristics and tumor angiogenesis. *Oncol Rep*. 2007;18:361-367.
 79. Masin M, Vazquez J, Rossi S, et al. GLUT3 is induced during epithelial-mesenchymal transition and promotes tumor cell proliferation in non-small cell lung cancer. *Cancer Metab*. 2014;2:11.
 80. Lu P, Takai K, Weaver VM, Werb Z. Extracellular matrix degradation and remodeling in development and disease. *Cold Spring Harb Perspect Biol*. 2011;3:a005058.
 81. Xiong G-F, Xu R. Function of cancer cell-derived extracellular matrix in tumor progression. *J Cancer Metastasis Treat*. 2016;2:357-364.
 82. Levental KR, Yu H, Kass L, et al. Matrix crosslinking forces tumor progression by enhancing integrin signaling. *Cell*. 2009;139:891-906.
 83. Arnold SA, Rivera LB, Miller AF, et al. Lack of host SPARC enhances vascular function and tumor spread in an orthotopic murine model of pancreatic carcinoma. *Dis Model Mech*. 2010;3:57-72.
 84. Fang M, Yuan J, Peng C, Li Y. Collagen as a double-edged sword in tumor progression. *Tumour Biol*. 2014;35:2871-2882.

85. Blumenthal RD, Leon E, Hansen HJ, Goldenberg DM. Expression patterns of CEACAM5 and CEACAM6 in primary and metastatic cancers. *BMC Cancer*. 2007;7:2.
86. Johnson B, Mahadevan D. Emerging role and targeting of carcinoembryonic antigen-related cell adhesion molecule 6 (CEACAM6) in human malignancies. *Clin Cancer Drugs*. 2015;2:100-111.
87. Ranjan Nath P. Peptidyl-prolyl isomerase (PPIase): an emerging area in tumor biology. *Cancer Res Front*. 2017;3:126-143.
88. Kang SA, Lee ES, Yoon HY, Randazzo PA, Lee ST. PTK6 inhibits down-regulation of EGF receptor through phosphorylation of ARAP1. *J Biol Chem*. 2010;285(34):26013-26021.
89. Yoon H-Y, Lee J-S, Randazzo PA. ARAP1 regulates endocytosis of EGFR. *Traffic*. 2008;9:2236-2252.
90. Zhao X, Chen M, Tan J. Knockdown of ZFR suppresses cell proliferation and invasion of human pancreatic cancer. *Biol Res*. 2016;49:26.
91. Zhang H, Zhang CF, Chen R. Zinc finger RNA-binding protein promotes non-small-cell carcinoma growth and tumor metastasis by targeting the Notch signaling pathway. *Am J Cancer Res*. 2017;7:1804-1819.
92. Cao W, Ma E, Zhou L, Yuan T, Zhang C. Exploring the FGFR3-related oncogenic mechanism in bladder cancer using bioinformatics strategy. *World J Surg Oncol*. 2017;15:66.
93. Scheller U, Pfisterer K, Uebe S, et al. Integrative bioinformatics analysis characterizing the role of EDC3 in mRNA decay and its association to intellectual disability. *BMC Med Genomics*. 2018;11:41.
94. Ghosh S, Jacobson A. RNA decay modulates gene expression and controls its fidelity. *Wiley Interdiscip Rev RNA*. 2010;1:351-361.
95. Li Y, Kiledjian M. Regulation of mRNA decapping. *Wiley Interdiscip Rev RNA*. 2010;1:253-265.
96. Wu C, Liu W, Ruan T, Zhu X, Tao K, Zhang W. Overexpression of mRNA-decapping enzyme 1a affects survival rate in colorectal carcinoma. *Oncol Lett*. 2018;16:1095-1100.
97. Grudzien-Nogalska E, Jiao X, Song M-G, Hart RP, Kiledjian M. Nudt3 is an mRNA decapping enzyme that modulates cell migration. *RNA*. 2016;22:773-781.
98. Reaves ML, Young BD, Hosios AM, Xu Y-F, Rabinowitz JD. Pyrimidine homeostasis is accomplished by directed overflow metabolism. *Nature*. 2013;500:237-241.
99. Li L, Fridley B, Kalari K, et al. Gemcitabine and cytosine arabinoside cytotoxicity: association with lymphoblastoid cell expression. *Cancer Res*. 2008;68:7050-7058.
100. Al-Haj L, Khabar KSA. The intracellular pyrimidine 5'-nucleotidase NT5C3A is a negative epigenetic factor in interferon and cytokine signaling. *Sci Signal*. 2018;11:eaal2434.
101. Colotta F, Allavena P, Sica A, Garlanda C, Mantovani A. Cancer-related inflammation, the seventh hallmark of cancer: links to genetic instability. *Carcinogenesis*. 2009;30:1073-1081.
102. Hsu C-H, Hsu C-W, Hsueh C, et al. Identification and characterization of potential biomarkers by quantitative tissue proteomics of primary lung adenocarcinoma. *Mol Cell Proteomics*. 2016;15:2396-2410.
103. Kawamura T, Nomura M, Tojo H, et al. Proteomic analysis of laser-microdissected paraffin-embedded tissues: (1) stage-related protein candidates upon non-metastatic lung adenocarcinoma. *J Proteomics*. 2010;73:1089-1099.
104. Kim YJ, Sertamo K, Pierrard M-A, et al. Verification of the biomarker candidates for non-small-cell lung cancer using a targeted proteomics approach. *J Proteome Res*. 2015;14:1412-1419.
105. Perez-Riverol Y, Csordas A, Bai J, et al. The PRIDE database and related tools and resources in 2019: improving support for quantification data. *Nucleic Acids Res*. 2019;47:D442-D450.
106. Shen W, et al. ICAM3 mediates tumor metastasis via a LFA-1-ICAM3-ERM dependent manner. *Biochim Biophys Acta - Mol Basis Dis*. 2018;1864:2566-2578.
107. Muñoz-Sánchez J, Cháñez-Cárdenas ME. A Review on Hemeoxygenase-2: Focus on Cellular Protection and Oxygen Response. *Oxid Med Cell Longev*. 2014;1-16.
108. Liu Y-Z, Wang B-S, Jiang Y-Y, et al. MCMs expression in lung cancer: implication of prognostic significance. *J Cancer*. 2017;8(18):3641-3647.
109. Liu Y-Z, Jiang Y-Y, Wang B-S, et al. A panel of protein markers for the early detection of lung cancer with bronchial brushing specimens. *Cancer Cytopathol*. 2014;122(11):833-841.
110. Xu H, Ma J, Wu J, et al. Gene expression profiling analysis of lung adenocarcinoma. *Braz J Med Biol Res*. 2016;49(3).
111. Li J, Zhang N, Zhang R, et al. CDC5L Promotes hTERT Expression and Colorectal Tumor Growth. *Cell Physiol Biochem*. 2017;41 (6):2475-2488.
112. Li X, Wang X, Song W, et al. Oncogenic Properties of NEAT1 in Prostate Cancer Cells Depend on the CDC5L-AGRN Transcriptional Regulation Circuit. *Cancer Res*. 2018;78 (15):4138-4149.
113. Huang R, Xue R, Qu D, Yin J, Shen X-Z. Prp19 Arrests Cell Cycle via Cdc5L in Hepatocellular Carcinoma Cells. *Int J Mol Sci*. 2017;18 (4):778.
114. Kumar A, Kumar Dorairaj S, Prabhakaran VC, Prakash DR, Chakraborty S. Identification of genes associated with tumorigenesis of meibomian cell carcinoma by microarray analysis. *Genomics*. 2007;90 (5):559-566.
115. Zhao H, Guo E, Hu T, et al. KCNN4 and S100A14 act as predictors of recurrence in optimally debulked patients with serous ovarian cancer. *Oncotarget*. 2016;7 (28):43924-43938.
116. Qian J, Ding F, Luo A, Liu Z, Cui Z. Overexpression of S100A14 in human serous ovarian carcinoma. *Oncol Lett*. 2016;11 (2):1113-1119.
117. Ehmsen S, Hansen LT, Bak M, Brasch-Andersen C, Ditzel HJ, Leth-Larsen R. S100A14 is a novel independent prognostic biomarker in the triple-negative breast cancer subtype. *Int J Cancer*. 2015;137 (9):2093-2103.
118. Zhao F-T, Jia Z-S, Yang Q, Song L, Jiang X-J. S100A14 Promotes the Growth and Metastasis of Hepatocellular Carcinoma. *Asian Pac J Cancer P*. 2013;14 (6):3831-3836.
119. Ding F, Wang D, Li X-K, et al. Overexpression of S100A14 contributes to malignant progression and predicts poor prognosis of lung adenocarcinoma. *Thorac Cancer*. 2018;9 (7):827-835.
120. Katono K, Sato Y, Kobayashi M, et al. Clinicopathological Significance of S100A14 Expression in Lung Adenocarcinoma. *Oncol Res Treat*. 2017;40 (10):594-602.
121. Sharma S, Langhendries J-L, Watzinger P, Kötter P, Entian K-D, Lafontaine DLJ. Yeast Kre33 and human NAT10 are conserved 18S rRNA cytosine acetyltransferases that modify tRNAs

- assisted by the adaptor Tan1/THUMPD1. *Nucleic Acids Res.* 2015;43 (4):2242–2258.
122. Zhang X, Jiang G, Sun M, et al. Cytosolic THUMPD1 promotes breast cancer cells invasion and metastasis via the AKT-GSK3-Snail pathway. *Oncotarget.* 2017;8 (8):13357–13366.
123. Huang Y, Chu T, Liao T, Hu X, Huang B. Downregulation of lysosomal and further gene expression characterization in lung cancer patients with bone metastasis. *Artif Cells Nanomed Biotechnol.* 2017;45 (4):758–764.
124. Keng VW, Villanueva A, Chiang DY, et al. A conditional transposon-based insertional mutagenesis screen for genes associated with mouse hepatocellular carcinoma. *Nat Biotechnol.* 2009;27 (3):264–274.
125. Zender L, Villanueva A, Tovar V, Sia D, Chiang DY, Llovet JM. Cancer gene discovery in hepatocellular carcinoma. *J Hepatol.* 2010;52 (6):921–929.
126. Zhu Y-C, Wang W-X, Song Z-B, et al. MET-UBE2H Fusion as a Novel Mechanism of Acquired EGFR Resistance in Lung Adenocarcinoma. *J Thorac Oncol.* 2018;13 (10):e202–e204.
127. Zheng Y-Z, Liang L. High expression of PXDN is associated with poor prognosis and promotes proliferation, invasion as well as migration in ovarian cancer. *Ann. Diagn Pathol.* 2018;34 161–165.

SUPPORTING INFORMATION

Additional supporting information may be found online in the Supporting Information section at the end of the article.

How to cite this article: Kelemen O, Pla I, Sanchez A, et al. Proteomic analysis enables distinction of early- versus advanced-stage lung adenocarcinomas. *Clin Transl Med.* 2020;10:e106. <https://doi.org/10.1002/ctm2.2106>